Journal of Instrumentation

Temperature analysis in the shock waves regime for gas-filled plasma capillaries in plasma-based accelerators

Published by IOP Publishing for Sissa Medialab

Received: *January 6, 2019*
Revised: *February 22, 2019*
Accepted: *February 25, 2019*
Published: *March 7, 2019*

5TH International Conference Frontiers in Diagnostcs Technologies
3–5 October 2018
INFN Frascati, Rome, Italy

Temperature analysis in the shock waves regime for gas-filled plasma capillaries in plasma-based accelerators

A. Biagioni,[a,1] **D. Alesini,**[a] **M.P. Anania,**[a] **M. Bellaveglia,**[a] **S. Bini,**[a] **F. Bisesto,**[a] **E. Brentegani,**[a] **E. Chiadroni,**[a] **A. Cianchi,**[b] **O. Coiro,**[a] **G. Costa,**[a] **M. Croia,**[a] **A. Del Dotto,**[a] **D. Di Giovenale,**[a] **G. Di Pirro,**[a] **M. Ferrario,**[a] **F. Filippi,**[a] **A. Giribono,**[a] **V. Lollo,**[a] **A. Mostacci,**[c] **D. Pellegrini,**[a] **R. Pompili,**[a] **S. Romeo,**[a] **J. Scifo,**[a] **V. Shpakov,**[a] **A. Stella,**[a] **C. Vaccarezza,**[a] **F. Villa**[a] **and A. Zigler**[d]

[a] *Laboratori Nazionali di Frascati, INFN, Via E. Fermi 40, 00044 Frascati, Italia*
[b] *Dipartimento di Fisica, Università di Roma Tor Vergata, V. della Ricerca Scientifica 1, 00133 Roma, Italia*
[c] *Dipartimento di Scienze di Base e Applicate per l'Ingegneria (SBAI), Sapienza Università di Roma, Via A. Scarpa 14–16, 00161 Roma, Italia*
[d] *Hebrew University of Jerusalem, Jerusalem 91904, Israel*

E-mail: Angelo.Biagioni@lnf.infn.it

Abstract: Plasma confinement represents a crucial point for plasma-based accelerators and plasma lenses because it can strongly affect the beam properties. For this reason, an accurate measurement of the plasma parameters, as plasma temperature, pressure and electron density, must be performed. In this paper, we introduce a novel method to detect the plasma temperature and the pressure for gas-filled capillaries in use at the SPARC_LAB test facility. The proposed method is based on the shock waves produced at the ends of the capillary during the gas discharge and the subsequent plasma formation inside it. By measuring the supersonic speed of the plasma outflow, the thermodynamic parameters have been obtained both outside and inside the capillary. A plasma temperature around 1.4 eV has been measured, that depends on the geometric properties and the operating conditions of the capillary.

Keywords: Plasma diagnostics - high speed photography; Wake-field acceleration (laser-driven, electron-driven); Accelerator Applications; Plasma diagnostics - charged-particle spectroscopy

[1] Corresponding author.

https://doi.org/10.1088/1748-0221/14/03/C03002

2019 JINST 14 C03002

Contents

2019 JINST 14 C03002

1 Introduction

The strong interest in the development of compact accelerator machines to go over the limits of the conventional accelerators [1] is leading towards plasma-based devices able to produce accelerating gradients in the GV/m scale [2, 3]. Such plasma-based structures can be also used to focus charged particle beams with large energies. For these reasons, these new compact devices are currently replacing conventional accelerators [4–6] and standard focusing devices [7–9]. In this regard, recently, several proof of principle experiments have been performed in focusing electron beams by means of active plasma lenses [10–13], consisting of gas-filled capillaries in which the plasma is produced by an electrical discharge [14, 15]. In this context, the activity of the SPARC_LAB [16] test-facility (LNF-INFN, Frascati) is currently focused on the development of new plasma-based accelerators. Here a gas-filled capillary plasma source is going to be used, whose plasma properties measurement is required. Temperature, pressure and plasma density, inside and outside the capillary plasma source, represent essential parameters that have to be investigated to understand the plasma evolution and how it can affect the electron beam passing through it.

With this aim, we present a novel method to estimate temperature and pressure inside the capillary, based on the study of free axisymmetric expansion of plasma from its orifices into the vacuum. This kind of thermodynamic analysis will be performed in terms of the local Mach number in the shock regions, also called plasma plumes, created at the exits of the capillary [17–20]. In these areas, the gas mixture composed of electrons, neutral molecules and ions, expands from the capillary into a very low pressure background (the capillary is placed inside a vacuum chamber), causing the shock formation which is propagating at different outflow velocities depending on the thermodynamic properties of the gas: temperature, pressure and density, which can be modified by changing the discharge voltage applied to the capillary in order to produce the plasma. In this paper, we report the thermodynamic study which is performed by measuring the plasma outflow velocities in the shock waves regime.

2 Theory

Supersonic gas expansions will be produced if the particles propagate faster than the sound speed corresponding to the gas temperature, that is the characteristic speed defined as $c = (\gamma_{H_2} R_s T)^{1/2}$, as a consequence of the pressure difference $\Delta p = p_i - p_e$ between internal and external pressures of the capillary. The parameter $\gamma_{H_2} = C_p/C_v$ is the heat capacity ratio, R_s and T are the specific gas constant and the gas temperature, respectively. Typically, during the supersonic expansion, in the shock regime formation, the outflow velocity u will increase because the thermal energy of the gas inside the capillary is converted in kinetic energy when it goes into vacuum, since this process can be considered as an adiabatic phenomenon. At the same time, the gas temperature decreases and therefore the characteristic sound speed will decrease along the plume axis. Such a typical behaviour of the shock wave creation has to be described by using the Mach number Ma, that is defined as the ratio between the gas outflow velocity u and the characteristic speed of sound, $Ma = u/c$; for this reason, this parameter will increase while the plasma plume expands. The expansion velocity of the plumes in the vacuum can be obtained as the ratio between the distance from the orifice of wavefronts and the corresponding delay time [21]. In the shock wave regime, the plume propagation follows a nonlinear behaviour [22], that is the gas outflow velocity u grows towards an asymptotic value u_∞ that represents the thermodynamic limiting velocity (corresponding to $Ma \to \infty$), which is defined as [23–25]:

$$u_\infty = \sqrt{2R_s \left(\frac{\gamma_{H_2}}{\gamma_{H_2} - 1}\right) T_0} \tag{2.1}$$

where T_0 is the temperature inside the capillary that we want to detect and $\gamma_{H_2} = 7/5$. In the shock regime, the Mach number Ma relates pressure, temperature, density and gas speed, as shown by the equations below [26, 27]:

$$\frac{T}{T_0} = \left(1 + \frac{\gamma_{H_2} - 1}{2} Ma^2\right)^{-1}, \tag{2.2}$$

$$\frac{\rho}{\rho_0} = \left(1 + \frac{\gamma_{H_2} - 1}{2} Ma^2\right)^{\frac{-1}{\gamma_{H_2} - 1}}, \tag{2.3}$$

$$\frac{p}{p_0} = \left(1 + \frac{\gamma_{H_2} - 1}{2} Ma^2\right)^{\frac{-\gamma_{H_2}}{\gamma_{H_2} - 1}}. \tag{2.4}$$

The physical quantities ρ_0 and p_0 are density and pressure inside the capillary, but ρ and p indicate the same quantities outside the capillary. It has been shown that the inner temperature T_0 can be calculated from eq. (2.1), so the external one, T, can be obtained by using the eq. (2.2), once we know Ma. The parameter Ma can be evaluated from eq. (2.3) because the plasma densities inside and outside the capillary, ρ_0 and ρ respectively, have been estimated by using the Stark broadening technique [28, 29].

3 Experimental setup

Figure 1 shows the experimental set-up we have used to acquire the images of plasma plume expansions (from which it is possible to detect the shock wavefronts) at the ends of the capillary.

2019 JINST 14 C03002

The experimental set-up uses cylindrical hydrogen-discharge plasma capillaries. The channel achieved inside the capillary (capillary's channel), where the plasma has been confined, is 30 mm in length and 0.5 mm in radius. Two gas inlets of 0.3 mm in radius feed this channel with hydrogen gas.

The discharge circuit provides the power supply to produce the current discharge within the capillary by means of a high-voltage switch and a delay generator (Stanford Research DG535) to synchronize all events: gas injection, image acquisition by using a gated intensified CCD camera (ANDOR iStar 320T), which is placed perpendicular to the plasma plume expansion, and supplying high-voltage to produce the gas ionization [32]. The timing that has been used to produce the plasma inside the capillary is the following. The gas valve is kept open for 3 ms to inject the hydrogen gas inside the capillary's channel; subsequently, 10 µs from the falling time, the high-voltage pulse is applied to the electrodes to ionize the gas and create the plasma within the channel.

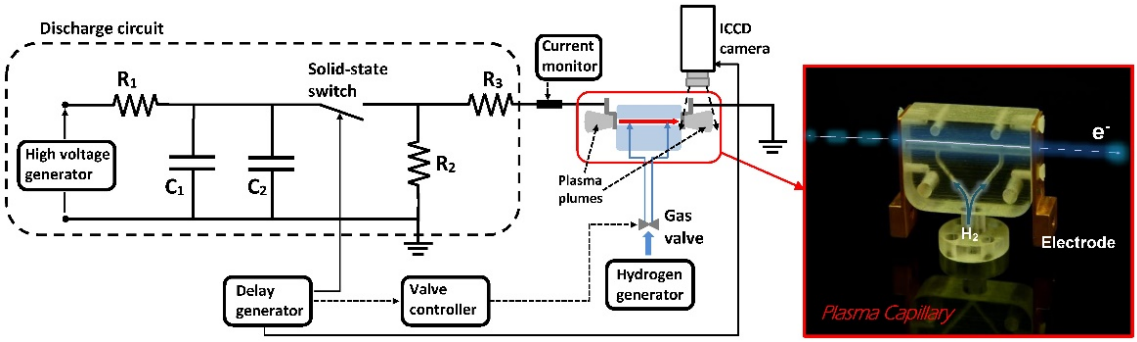

Figure 1. Experimental set-up used to ionize the hydrogen gas inside the capillary and to measure the plasma properties by using the shock formation to its ends. Circuit parameters: $R_1 = 10\,\mathrm{k\Omega}$; $R_2 = 400\,\mathrm{k\Omega}$; $R_3 = 38\,\Omega$; $C_1 = C_2 = 3.6\,\mathrm{nF}$.

In order to measure the gas outflow velocity (plasma velocity) downstream the orifices of the capillary's channel, we have acquired several images of the plasma plumes at different instants of time, that have to be synchronized with the beginning of the current discharge, $t_0 = 0$, inside the capillary's channel. These images have been taken with increasing delay times t_D with steps of 50 ns, starting from $t_D = t_0$ of up to 2000 ns, to describe the shock wave formation outside the capillary. The exposure time of the ICCD camera has been set to 5 ns.

4 Results

The gas expansion in the shock waves regime is represented in figure 2. It shows three different examples of plasma plumes corresponding to different delay times from t_0. Also, figure 2d shows the longitudinal profile along z-direction related to a delay time $t_D = 900$ ns (figure 2c), that is used to identify the wavefront of the plasma plumes.

The asymptotic value is $u_\infty = y_0 \approx 21300 \pm 420$ m/s when the discharge voltage is set to 18 kV, that is the y_0 term of the exponential fit shown in figure 3a. It should be noted that the maximum expansion length is around 25 mm, relating to a delay time of 1350 ns. Therefore, from eq. (2.1) we obtain $T_0 \approx 1.4 \pm 0.05$ eV. Such value represents the average plasma temperature inside and on axis of the plasma channel, but nearby its extremities.

2019 JINST 14 C03002

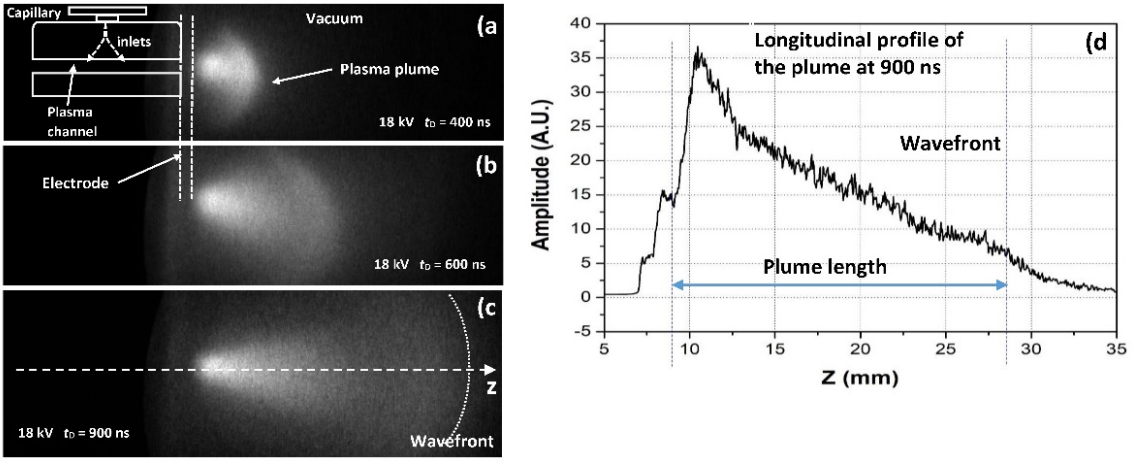

Figure 2. (a)–(c) Plasma plume temporal evolution produced at the exits of the capillary when the discharge voltage is 18 kV. (d) Longitudinal profile of the plasma plume related to a delay time $t_D = 900$ ns.

In this conditions, the characteristic speed of sound corresponding to the temperature $T_0 = 1.4$ eV is $c = (\gamma_{H_2} R_s T_0)^{1/2} \approx 9400 \pm 250$ m/s, that represents also the gas propagation velocity inside the capillary supposing it expands at sonic regime ($Ma = 1$). On the contrary, the gas outflow from the orifices occurs in the shock regime ($Ma > 1$), so the real expansion velocity u of the plasma plumes will be different from the characteristic speed of sound c in such regions, since they are connected by the Mach number.

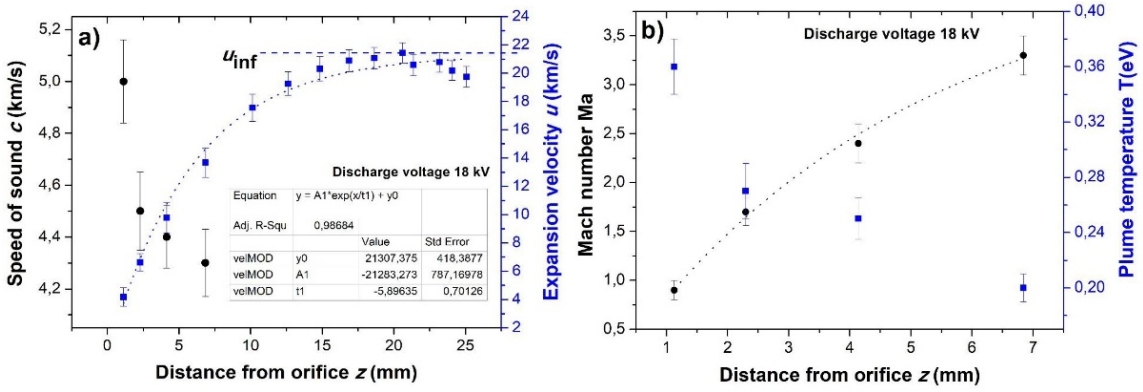

Figure 3. Shock regime description: a) measured expansion velocity of the gas u (blue squares) and characteristic speed of sound c (black circles) as a function of the distance from the orifice that the wavefront has reached; b) Mach number and temperature within the plasma plume as a function of the distance from the orifice.

The speed of sound c obtained from the temperature T in the shock regions is again plotted in figure 3a (black circles). It would be the gas expansion velocity if it propagated at sonic regime. It should be noted that the first measured value of c is around 5000 ± 180 m/s, corresponding to 1.1 mm from the orifice. Also, the first four values of c, up to 6.8 mm from the orifice (corresponding to a delay time of 650 ns), highlight a decreasing of the speed of sound while the measured expansion

2019 JINST 14 C03002

velocity u is increasing. In our experimental conditions, as will be explained below, the speed of sound relating to expansion lengths larger than about 6.8 mm cannot be evaluated.

The estimation of the Mach number Ma has been performed by using the Stark broadening method. Figure 4a shows the spectrum curves of the hydrogen Balmer alpha line, H_α (λ = 656.3 nm), that we have obtained through the Stark broadening measurements of the plasma inside our capillary. From these spectrum profiles, we can know the electron density of the plasma by width of the Stark-broadened H_α [30, 31]: the larger is the spectral line-width of H_α, the higher is the electron density produced by the high-voltage discharge; in fact, the relationship is given by:

$$n_e = 8.02 \times 10^{12} \left(\frac{\Delta\lambda}{\alpha}\right)^{\frac{3}{2}} \text{ cm}^{-3}, \tag{4.1}$$

where $\Delta\lambda$ represents the FWHM of the spectral curve in angstroms and α is a tabulated parameter that is different for each Balmer line [29]. These spectral curves have been obtained by collecting the light emitted by the ionized hydrogen with an optical system, which is sent to an imaging spectrometer (SpectraPro275) with a 2400 g/mm grating. Therefore, by using the ICCD camera (255×1024 pixels) to acquire the spectrally dispersed plasma light, we obtain a broadened spectral line that is spatially-resolved along the shorter dimension of the ICCD camera, with a resolution around 80 μm per pixel (in this imaging system, that direction represents the longitudinal dimension of the capillary). However, it should be noted that to measure the expansion velocity of the plasma plumes, the spectrometer has to be removed and only the ICCD camera is used to acquire the images of the plume at different delay times.

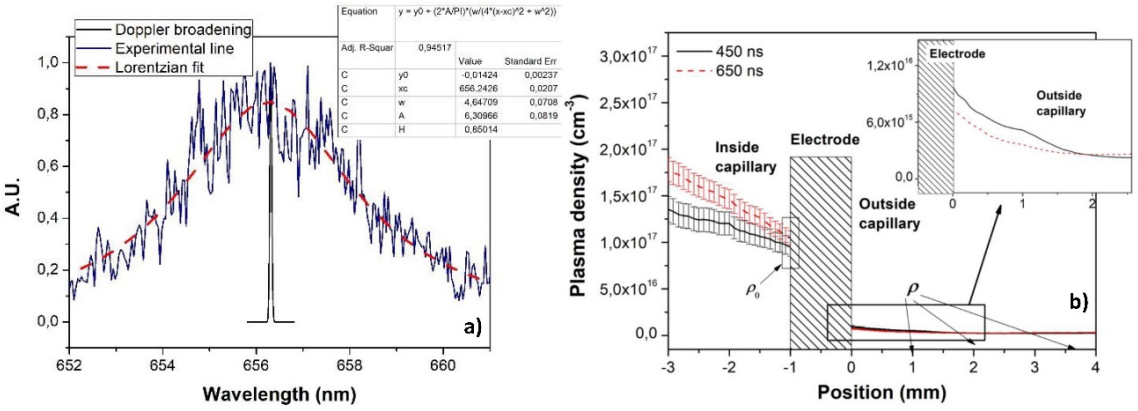

Figure 4. Density measurements by using the Stark broadening method: a) spectrum curves of the hydrogen Balmer alpha line, H_α, corresponding to 656.3 nm (blue line) together with the Lorentzian fit (red dashed line) and the Doppler broadening for a plasma temperature of 2 eV (black line). b) density profiles measured at different delay times as a function of the position in the capillary; in particular, it shows some positions surrounding the electrode, where the thermodynamic properties of the plume have been obtained. The shot-to-shot standard deviation errors represented by the error bars are obtained by analyzing 100 shots.

The spectral lines are subjected to broadening caused by two different effects: the Stark effect, which is proportional to the electron density, and the Doppler broadening due to the thermal motion of the particles, that depends on the plasma temperature. In our conditions, the plasma temperature is lower than 2 eV, therefore, the Doppler broadening contribution is around 0.1 nm FWHM, that

2019 JINST 14 C03002

can be neglected with respect to the Stark effect contribution, which reaches around 4 nm FWHM (figure 4a). It should be noted that, for this reason, the experimental lines measured by using the Stark broadening method can be fitted with a Lorentzian curve. Figure 4b shows the density profiles along the longitudinal axis of the capillary concerning two different delay times, 450 and 650 ns, that we have obtained by the processing of the spectral curves.

The density profiles have been used to estimate Ma (eq. (2.3)), the downstream temperature T (eq. (2.2)) and so the characteristic speed of sound c along the longitudinal axes of the plasma plume. It should be noted that plasma densities cannot be measured at distances larger than around 6.8 mm because beyond such value the SNR becomes too low (for densities lower than 10^{15} cm^{-3}). However, data reported in figure 3 provide a correct characterization of the shock regime. In fact, Ma acquires increasing values while the expansion velocity u grows exponentially toward an asymptotic value, and, at the same time, c decreases along the longitudinal axis because also the downstream temperature T decreases along this axis. Finally, by using eq. (2.4) it is also possible to obtain the pressure values inside and outside the capillary. The average inner pressure, close to the plasma channel extremities, is 150 ± 15 mbar, while after 1 mm outside the capillary it is already become 2.5 ± 0.08 mbar, when the discharge voltage is 18 kV.

5 Conclusions

Gas-filled capillary plasma sources represent a typical solution to confine a plasma for plasma-based accelerators. In these devices, the gas ionization, and so the plasma properties, can be affected by the fluid dynamics behaviour along the capillary's channel. In particular, in this work we have analysed the shock wave regime created at the ends of the capillary to evaluate the temperature and, consequently, other thermodynamic properties of plasma which in turn affect the beam dynamics. In fact, in our measurements, the shock regions, caused by the gas expansion into the vacuum through the capillary's orifices, occupy about 40 mm in length (20 mm each one), that is longer than the capillary length, even if at different operating conditions. The shock waves formation has been proved by measuring the gas outflow velocities, that show a typical exponential growth towards an asymptotic value, then used to estimate the inner temperature of the plasma. With this method it is possible to evaluate such temperature as a function of the discharge voltages applied to the capillary, that in our measurements is around 1.4 eV at 18 kV of the voltage. Also, the average inner pressure is around 150 mbar at the same value of the discharge voltage. In the shock regions, also the measurements of speed of sound, Mach number, downstream temperature and pressure are in agreement with such a regime. Finally, it should be considered that such an analysis could also be made inside the capillary to evaluate temperature and pressure along its longitudinal axes, by measuring the expansion velocities at the beginning of the plasma creation.

Acknowledgments

This work was supported by the European Unions Horizon 178 2020 research and innovation programme under grant agreement No. 653782.

2019 JINST 14 C03002

References

[1] M. Reiser, *Theory and design of charged particle beams*, John Wiley & Sons (2008).

[2] T. Tajima and J.M. Dawson, *Laser electron accelerator*, *Phys. Rev. Lett.* **43** (1979) 267.

[3] T. Hosokai, M. Kando, H. Dewa, H. Kotaki, S. Kondo, N. Hasegawa et al., *Optical guidance of terrawatt laser pulses by the implosion phase of a fast z-pinch discharge in a gas-filled capillary*, *Opt. Lett.* **25** (2000) 10.

[4] W.P. Leemans, B. Nagler, A.J. Gonsalves, C. Tóth, K. Nakamura, C.G.R. Geddes et al., *GeV electron beams from a centimetre-scale accelerator*, *Nat. Phys.* **2** (2006) 696.

[5] I. Blumenfeld et al., *Energy doubling of 42 GeV electrons in a metre-scale plasma wakefield accelerator*, *Nature* **445** (2007) 741.

[6] P.A. Walker et al., *Horizon 2020 EuPRAXIA Design Study*, *J. Phys. Conf. Ser.* **874** (2017) 012029.

[7] J.J. Su, T.C. Katsouleas, J.M. Dawson and R. Fedele, *Plasma lenses for focusing particle beams*, *Phys. Rev.* **A 41** (1990) 3321.

[8] E. Boggasch, A. Tauschwitz, H. Wahl, K.G. Dietrich, D.H.H. Hoffmann, W. Laux et al., *Plasma lens fine focusing of heavy-ion beams*, *Appl. Phys. Lett.* **60** (1992) 2475.

[9] G. Hairapetian, P. Davis, C.E. Clayton, C. Joshi, S.C. Hartman, C. Pellegrini et al., *Experimental demonstration of dynamic focusing of a relativistic electron bunch by an overdense plasma lens*, *Phys. Rev. Lett.* **72** (1994) 2403.

[10] R. Pompili et al., *Focusing of High-Brightness Electron Beams with Active-Plasma Lenses*, *Phys. Rev. Lett.* **121** (2018) 174801.

[11] J. van Tilborg et al., *Active Plasma Lensing for Relativistic Laser-Plasma-Accelerated Electron Beams*, *Phys. Rev. Lett.* **115** (2015) 184802.

[12] A. Marocchino, M.P. Anania, M. Bellaveglia, A. Biagioni, S. Bini, F. Bisesto et al., *Experimental characterization of the effects induced by passive plasma lens on high brightness electron bunches*, *Appl. Phys. Lett.* **111** (2017) 184101.

[13] R. Pompili, M. P. Anania, M. Bellaveglia, A. Biagioni, S. Bini, F. Bisesto et al., *Experimental characterization of active plasma lensing for electron beams*, *Appl. Phys. Lett.* **110** (2017) 104101.

[14] A. Butler, D.J. Spence and S.M. Hooker, *Guiding of High-Intensity Laser Pulses with a Hydrogen-Filled Capillary Discharge Waveguide*, *Phys. Rev. Lett.* **89** (2002) 185003.

[15] D.J. Spence, A. Butler and S.M. Hooker, *Gas-filled capillary discharge waveguides*, *J. Opt. Soc. Am.* **B 20** (2003) 138.

[16] M. Ferrario et al., *SPARC_LAB present and future*, *Nucl. Instrum. Meth.* **B 309** (2013) 183.

[17] H. Ashkenas, *Atomic beam scattering from single crystal surfaces*, in *Proceedings of the 4th International Symposium on Rarefied Gas Dynamics*, Vol. 2, Academic Press (1965), pp. 84–105.

[18] H.R. Murphy and D.R. Miller, *Effects of nozzle geometry on kinetics in free-jet expansions*, *J. Phys. Chem.* **88** (1984) 4474.

[19] F. Robben and L. Talbot, *Measurement of shock wave thickness by the electron beam fluorescence method*, *Phys. Fluids* **9** (1966) 633.

[20] G. Pham-Van-Diep, D. Erwin and E. P. Muntz, *Nonequilibrium molecular motion in a hypersonic shock wave*, *Science* **245** (1989) 624.

2019 JINST 14 C03002

[21] I. Mihaila, C. Ursu, A. Gegiuc and G. Popa, *Diagnostics of plasma plume produced by laser ablation using ICCD imaging and transient electrical probe technique*, *Jo. Phys. Conf. Ser.* **207** (2010) 012005.

[22] E.M. Rothkopf and W. Low, *Shock formation distance in a pressure driven shock tube*, *Phys. Fluids* **19** (1976) 1885.

[23] A. Naß and E. Steffens, *Direct Simulation of Low-Pressure Supersonic Gas Expansions and its Experimental Verification*, *Nucl. Instrum. Meth.* **A 598** (2009) 653 [arXiv:0810.0393].

[24] W. Christen, K. Rademann and U. Even, *Efficient cooling in supersonic jet expansions of supercritical fluids: CO and CO2*, *J. Chem. Phys.* **125** (2006) 174307.

[25] M. Reponen, I. Moore, I. Pohjalainen, T. Kessler, P. Karvonen, J. Kurpeta et al., *Gas jet studies towards an optimization of the IGISOL LIST method*, *Nucl. Instrum. Meth.* **A 635** (2011) 24.

[26] F. Saint-Laurent, G. Martin, T. Alarcon, A.L. Luyer, P. Pastor, S. Putvinski et al., *FIRE, a novel concept of massive gas injection for disruption mitigation in ITER: Validation on Tore Supra*, *Fusion Eng. Des.* **89** (2014) 3022.

[27] Ames Research Staff, *Equations, tables, and charts for compressible flow*, NACA Report 1135 (1953).

[28] A.J. Gonsalves, T.P. Rowlands-Rees, B.H.P. Broks, J.J.A.M. van der Mullen and S.M. Hooker, *Transverse interferometry of a hydrogen-filled capillary discharge waveguide*, *Phys. Rev. Lett.* **98** (2007) 025002.

[29] H.R. Griem and W.L. Barr, *Spectral line broadening by plasmas*, *IEEE Trans. Plasma Sci.* **3** (1975) 227.

[30] F. Filippi, M.P. Anania, E. Brentegani, A. Biagioni, A. Cianchi, E. Chiadroni et al., *Gas-filled capillaries for plasma-based accelerators*, *J. Phys. Conf. Ser.* **874** (2017) 012036.

[31] F. Filippi, M.P. Anania, A. Biagioni, E. Chiadroni, A. Cianchi, M. Ferrario et al., *Spectroscopic measurements of plasma emission light for plasma-based acceleration experiments*, 2016 *JINST* **11** C09015.

[32] M.P. Anania et al., *Plasma production for electron acceleration by resonant plasma wave*, *Nucl. Instrum. Meth.* **A 829** (2016) 254.

2019 JINST 14 C03002